

Development of co-Kriging based design optimisation methodology for a lean burn combustor

UTC for Computational Engineering

Moresh Wankhede, Neil Bressloff and Andy Keane, CEDG, School of Engineering Sciences

Marco Zedda, Rolls-Royce plc.

Introduction

Computational fluid dynamics (CFD) simulations are often used in the gas turbine industry to predict and visualize the reacting flow dynamics, combustion environment and emissions performance of a combustor at the design stage and to assess new concepts. The combustor's reacting flow-field is in general turbulent and embraces many complex fluid dynamic phenomena. Hence, the CFD simulation of a real gas turbine combustor is computationally very expensive. Given the complexity in obtaining accurate flow predictions and due to the expensive nature of simulations, conventional techniques for CFD based combustor design optimisation are often ruled out, primarily due to the limits on available computing resources and time. Surrogate-based design optimisation techniques (including Kriging meta-models) have been used previously to accelerate the design optimisation process by reducing the total number of expensive CFD analysis that would be necessary in direct search methods. In this study, we develop a computationally efficient co-Kriging based design optimisation strategy suitable for the design of a lean burn combustor using two levels of model analysis. This approach provides a means to achieve high-fidelity design optimisation at reduced cost by using a more accurate high-fidelity model in combination with a less accurate lower fidelity model (that is significantly less expensive to evaluate), both models being defined over the same design space.

Combustor model and reactive flow-field

A numerical study of turbulent reactive processes behind a profiled backward-facing step in a two-dimensional test combustion chamber is presented. The test combustor modeled for the study is the one used by Keller et al., 1982 and Ganji et al., 1980 in an experimental study of mechanisms of instabilities in turbulent combustion leading to flashback.

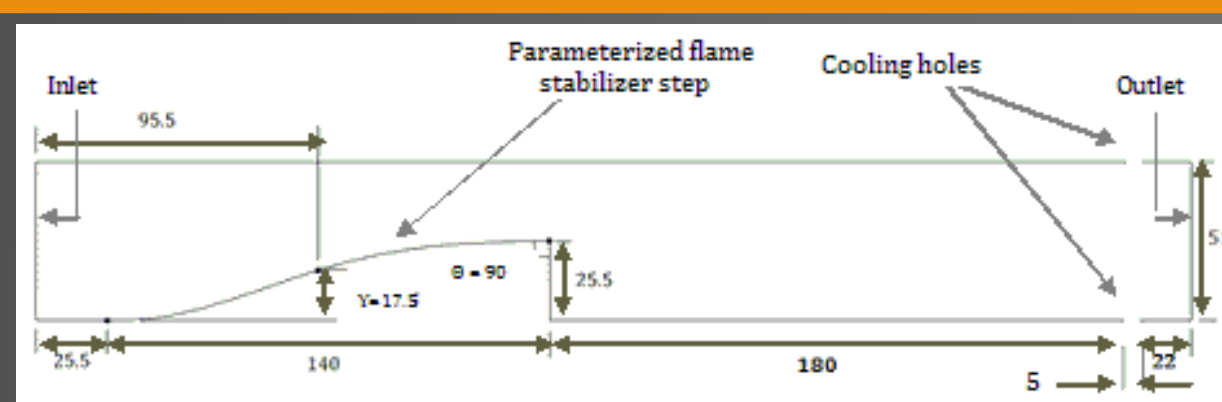


Figure 1. Computational domain of the combustor (All dimensions in mm)

Figure 1 shows the computational domain of the combustor with cooling holes near the outlet. The combustor consists of a profiled backward-facing step acting as the flame holder. A premixed lean propane/air mixture at equivalence ratio of 0.86 enters the combustor through the inlet at 13.3 m/s inlet-velocity and at atmospheric pressure. The cooling air enters through the cooling holes near the exit at 300 K. The cooling air enters at a 90 degrees angle to the reacting mixture flow inside the combustor.

For determining the effect of mesh size on the solution for the configuration shown in Figure 1, five meshes of increasing cell counts are constructed using GAMBIT 2.3. Table 1 lists the cell count on each mesh used and its run-time to convergence. A reactive steady RANS simulation of the domain (c.f. Figure 1) is run for all the five meshes and the temperature profiles at the exit plane are plotted.

Mesh	~ Cell Count	~Time (mins)
1	11,000	10
2	46,000	30
3	190,000	210
4	420,000	1080
5	800,000	2400

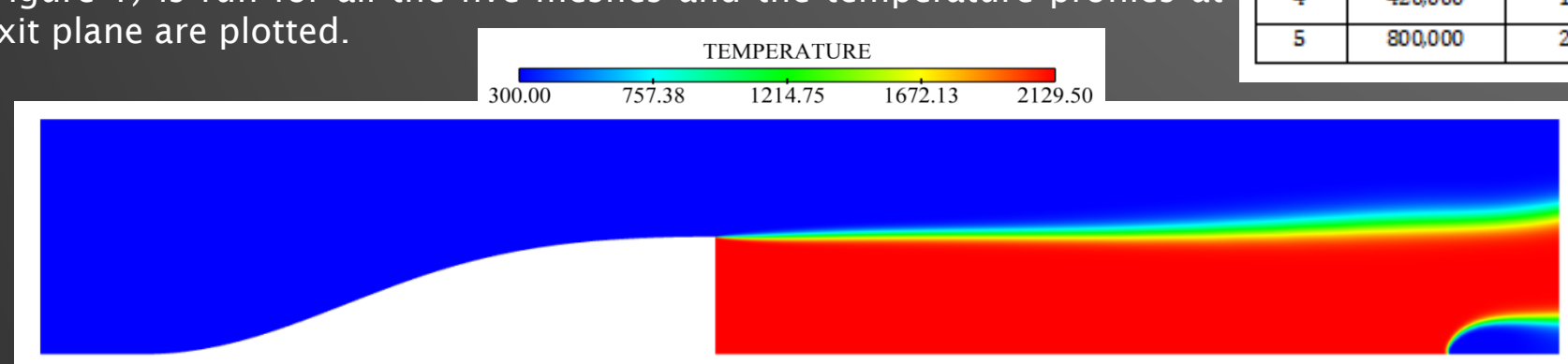


Figure 2. Position of the flame front behind the flame stabilizer step (steady RANS)

Figure 2 shows the position of the flame surface inside the chamber obtained using steady RANS and mesh 5. As the Reynolds number of the flow is in the turbulent regime, the mixture burns only in the location where the turbulent flame speed S_T is able to sustain the inlet mixture velocity, i.e. the region behind the step. Therefore the chamber behind the step is separated into unburnt and burnt mixture regions by an interface, where combustion has started but not yet fully established. Above this surface, $(C=0)$, the fuel and oxidizer mixture is mixed but unburnt, and below this surface $(C=1)$, the mixture is completely burnt.

Figure 3 shows the temperature profiles captured by different meshes at the exit plane of the combustor. Grid independence is closely approached by mesh 3, especially near the walls and within the burnt and unburnt zone of the combustor. However, near the flame front, the solution is not completely grid independent as higher number of cells are required to capture the flame front which also increases convergence run-time significantly. Hence from an engineering point of view and for the purpose of design optimisation, the profile captured by mesh 3 is selected as a feasible high-fidelity solution. For co-Kriging, profile captured by mesh 1 is used as the low-fidelity solution.

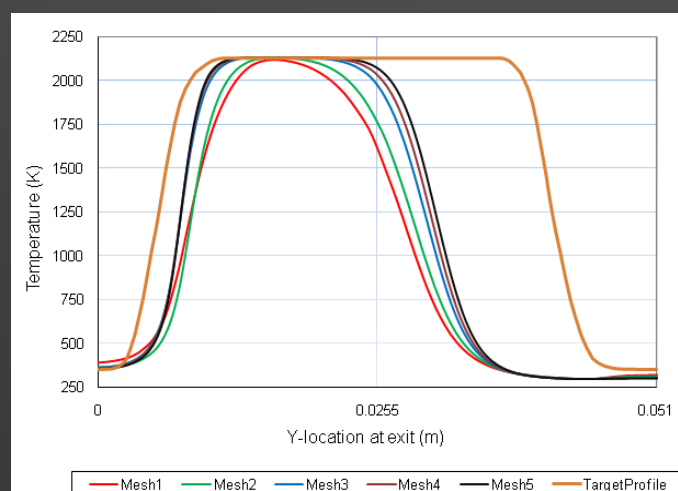


Figure 3. Temperature profiles at exit plane

Objective function and geometry parameterisation

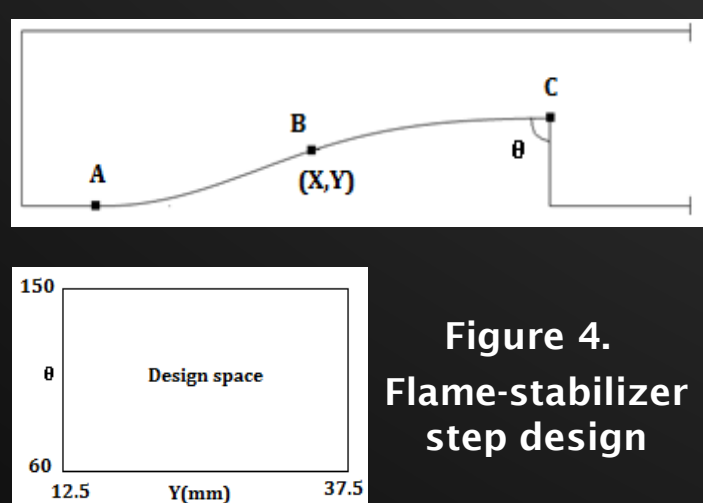


Figure 4. Flame-stabilizer step design

Figure 3 shows the desired exit temperature profile to be achieved by optimisation of the flame stabilizer step. The objective is to design the flame-stabilizer step whose exit temperature profile matches closely to the given target exit temperature profile. Root mean square deviation value is calculated for this purpose, between the observed temperature profile and the target temperature profile. The flame stabilizer step is constructed and parameterized using a cubic spline as shown in Figure 4. Points A, B and C are connected by a spline curve of which control point A and C are fixed. Y and θ are the two variables and the baseline design spline is defined at $Y = 17.5\text{mm}$ and $\theta = 90$ degrees.

Kriging based design optimisation

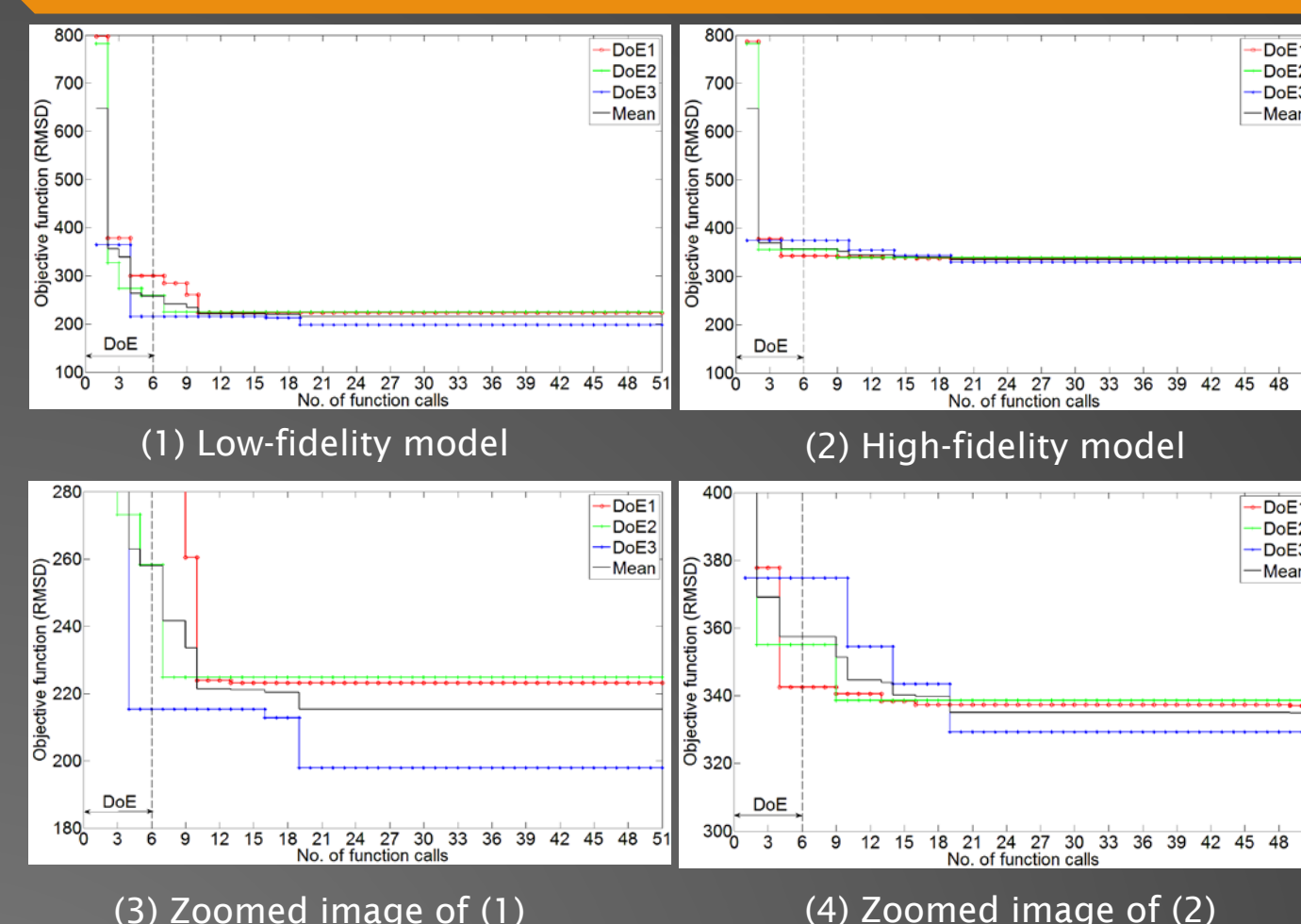


Figure 5. Optimisation history over a fixed computational budget of DoE + 15 update cycles

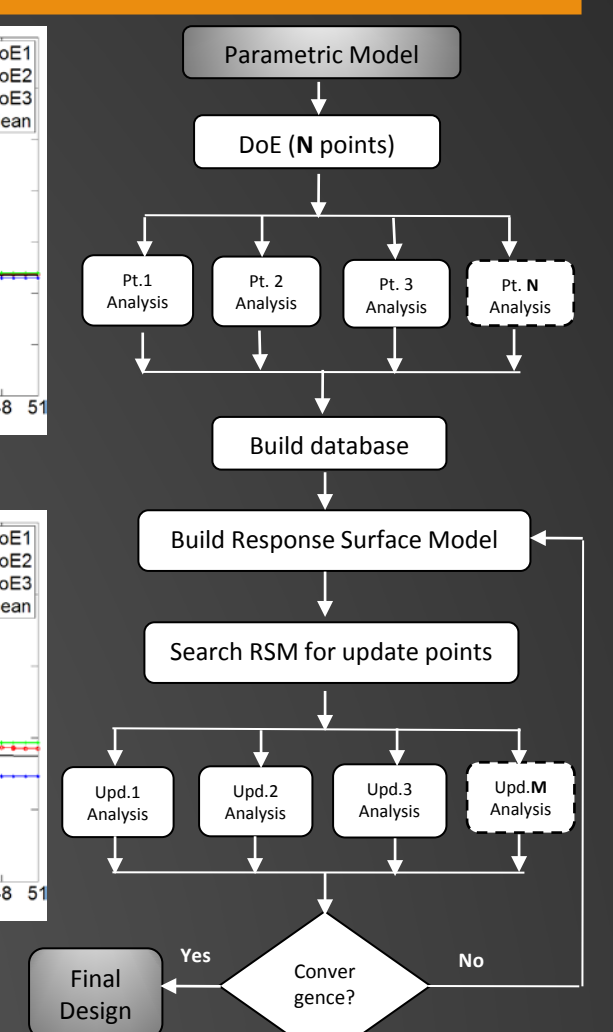


Figure 6. Kriging based optimisation

Figure 5 shows the optimisation history obtained using a Kriging based optimisation strategy (c.f. Figure 6) for both low and high fidelity models, over three different DoE samples. Starting with an initial set of 6 Latin Hypercube DoE points, the resulting objective function values are used to construct a Kriging meta-model. This model is then searched using genetic algorithm (GA) and then again using dynamic hill climbing (DHC) algorithm to find a series of three update points, each found using best predicted criterion, Kriging prediction error criterion and expected improvement criterion. These 3 CFD evaluations are carried out in each update cycle and the evaluated designs are then added to the existing database of results updating the Kriging model. As seen in Figure 5, the low-fidelity model under-predicts the objective function value as it is inaccurate.

The effect of different starting initial samples is also clearly seen in Figure 5, which generates different convergence histories leading to different optimums within the fixed computational budget. Figure 7 shows the optimum design obtained using high fidelity model over three DoE samples.

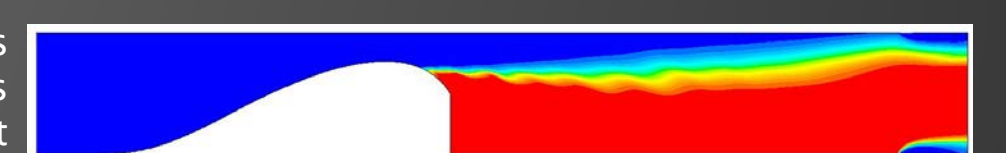


Figure 7. Optimum design using high fidelity model over three DoE samples

Co-Kriging based design optimisation

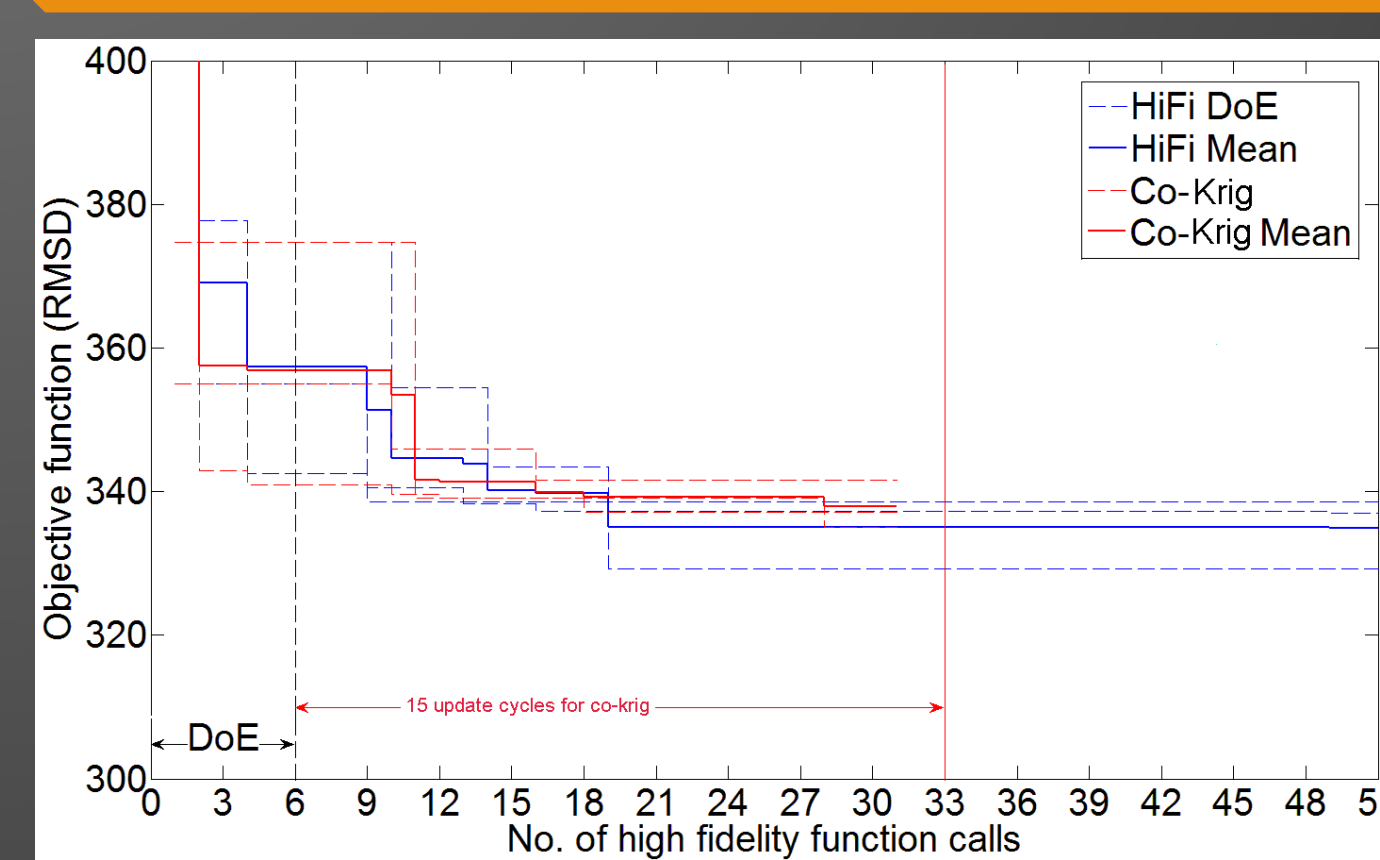


Figure 8. Optimisation history for co-Kriging and high fidelity model over three DoE samples

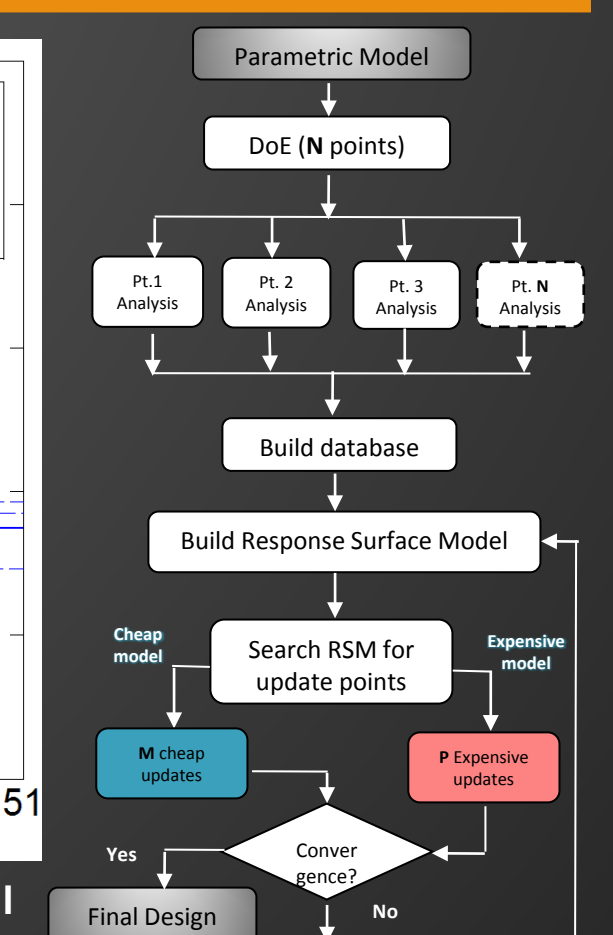


Figure 9. Co-Kriging strategy

Figure 8 shows the optimisation history for co-Kriging model obtained using a co-Kriging based optimisation strategy (c.f. Figure 9) along with high-fidelity model optimisation history over three different DoE samples. Initially, out of 6 DoE points, high fidelity CFD runs are carried out on 3 points and low-fidelity CFD runs are carried out on all 6 points. The resulting objective function values are used to construct a co-Kriging model, which is then searched to find three update points per cycle, each using best prediction, prediction error and expected improvement criteria. Out of these three update points, high-fidelity CFD runs are carried out on two update (best predicted and prediction error) points, whereas low-fidelity CFD runs are carried out on all three update points. This ratio of 3:2 update points CFD runs is utilized through out the 15 update cycles budget.

As seen in Figure 8, over three different DoE's, the mean of high-fidelity model optimisation history is lower than that of co-Kriging model, whereas the variance of the high-fidelity model is higher than that of co-Kriging model.

Future Work

The above developed co-Kriging optimisation system would be further explored using different number of initial samples and ratio of update points CFD runs and it is hoped that the optimum high fidelity design would be found in significantly less time as less number of high-fidelity function calls are required. The developed co-Kriging optimisation strategy would then be applied to an unsteady reactive CFD setup and the results would also be compared against the traditional Kriging based optimisation strategy. Finally, the fully developed and tested co-Kriging optimisation system would be applied to Rolls-Royce 3D lean burn injector optimisation problem.